Hindawi
International Journal of Antennas and Propagation
Volume 2023, Article ID 4988298, 6 pages
https://doi.org/10.1155/2023/4988298

Research Article

Optimized Surface Adjustment Method for Large Deployable Cable Network Antennas

Xin Zhang, Lipeng Wang, Xiaofei Ma, and Yizhe Wang

Xi'an Institute of Space Radio Technology, Xi'an, China

Correspondence should be addressed to Lipeng Wang; 624293993@qq.com

Received 7 May 2023; Revised 30 October 2023; Accepted 6 November 2023; Published 18 December 2023

Academic Editor: Claudio Gennarelli

Large deployable mesh reflectors typically require high surface accuracy and have large apertures. The accumulation of machining errors in a large number of cables can lead to significant deviations between the final manufactured surface and the theoretical surface, particularly due to the large number of cables involved. Adjusting the mesh reflector is often necessary to meet the surface accuracy requirements. However, traditional surface adjustment methods can be challenging to converge and time-consuming. To address this issue, our paper proposes an engineering surface based on measured manufacturing errors as a substitute for the theoretical surface. This method can save time on the coarse adjustment of surface accuracy for large deployable mesh reflectors, reducing the overall surface accuracy adjustment time by 30%.

1. Introduction

Large deployable mesh reflectors are widely used in communication satellites for their large apertures and low surface densities [1–3]. As shown in Figure 1, a typical cable network antenna comprises five parts [4, 5]: a ring-shaped deployable truss, a front cable network, a reflector mesh (usually a metal mesh), a rear cable network, and tension tie cables. The front and rear cable networks are, respectively, connected to the ring truss and tensioned by low-stiffness tension tie cables. The metal mesh is attached to the front network cables to form a high-precision paraboloid for sending and receiving electromagnetic signals [6]. Therefore, the front cable network of the mesh antenna requires high surface accuracy [7].

A large loop antenna typically consists of multiple parts, with apertures ranging from 5 meters to 50 meters [1, 2]. The surface error of the loop antenna is defined as the deviation between the manufactured reflective surface and the theoretical one [8], with the manufactured error being the dominant factor [3, 9]. The manufactured error arises during the machining and assembly of the antenna parts, and the accumulation of these errors leads to a significant gap between the manufactured and theoretical surfaces, even when the tolerance of individual parts is within acceptable limits. The error accumulates further as the aperture of the antenna increases. Consequently, there is a substantial challenge in achieving surface accuracy for large deployable loop antennas.

Various methods have been proposed for surface adjustment to decrease the manufactured error, including traditional approaches that adjust the length of the vertical cable and tension to improve the accuracy of the cable net reflective surface [10–12]. However, when the aperture of the deployable loop antenna exceeds 20 meters, the traditional surface adjustment methods become difficult to converge and are time-consuming due to the huge manufactured error.

In this paper, we analyze the manufactured error of large deployable loop antennas and propose an engineering surface as a substitute for the theoretical surface, based on the measured manufactured error. The engineering surface is obtained by converting the manufactured surface to the theoretical surface via surface adjustment and has the same gain as the theoretical surface in simulations. Compared to the theoretical surface, the engineering surface is much

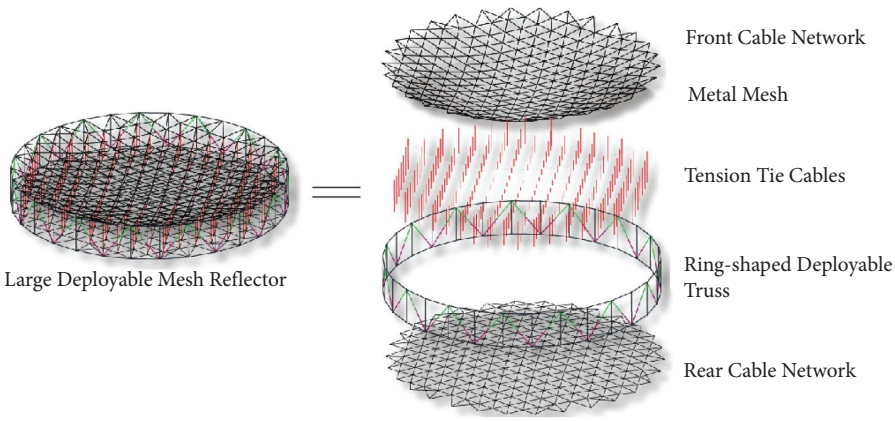

Figure 1: Composition of the deployable loop reflector.

easier to achieve through surface adjustment. This proposed method can significantly reduce the time required for surface adjustment of large deployable loop antennas.

2. Surface Adjustment Method

2.1. Manufacturing Error. The manufactured error of the large deployable loop antenna is mainly caused by part tolerances. It includes the following components:

(1) Deployable structure error (Δ_1): The deployable structure is assembled by many parallelogram units, as shown in Figure 2. The manufactured error includes length tolerances of the bars and assembly tolerances.

(2) Front (rear) cable network error (Δ_2): The front (rear) network is connected to the deployable structure, as shown in Figure 2. The manufactured error arises from the length tolerance of the ropes and length compensation, which is considered during the assembly process. The deployable structure of the loop antenna deforms when the front (rear) network is connected, making the actual length of the cable different from the designed length.

(3) Tension tie error (Δ_3): The tension tie connects the front network and the rear network. The manufactured error of the tension tie is the length tolerance.

Given the manufactured errors described above, there exists a large gap between the manufactured surface of the large deployable loop antenna and the theoretical surface. The deployable structure error is challenging to modify in practical engineering. The mesh antenna's cable network structure consists of thousands of cables. When the surface accuracy of the mesh antenna does not meet the requirements, it is typically necessary to adjust the lengths of the cables to achieve the desired reflective surface accuracy. This adjustment is complex due to the interdependence among the cables and the large number of ropes being adjusted. Therefore, surface adjustment aims to minimize the manufactured error by optimizing Δ_2 and Δ_3, as shown in the following equation:

$$\min\left\|S_t - S(\Delta_1, \Delta_2, \Delta_3)\right\|, \tag{1}$$

where s_t is the theoretical surface and $S(\Delta_1, \Delta_2, \Delta_3)$ is the adjusted surface.

2.2. Surface Accuracy. The reflective surface of the deployable loop antenna is approximated by triangular flat facets, as shown in Figure 3. The surface accuracy is measured using photogrammetry, and the root mean square (RMS) value is defined as the normal offset distance from the facet nodes to the theoretical surface. The RMS value is commonly used to quantify the surface accuracy of the deployable loop antenna:

$$\mathrm{RMS} = \frac{1}{n}\sum_{i=1}^{n}\sqrt{(S_t - p_i)^2}, \tag{2}$$

where s_t is the theoretical surface, p_i is the facet node, and n is the number of flat facets.

3. Improved Error-Based Surface Adjustment Method

The shape accuracy of the mesh antenna reflector is represented by the half-path-length best-fit RMS error between the measured surface of the front tension network and the surface of the standard paraboloid, as it directly affects the electrical performance of the mesh antenna. This involves two physical concepts, the half-path error and the best-fit paraboloid. As shown in Figure 4, when assuming that the electrical signal is reflected by the parabolic and triangular surfaces to the focal point, the optical path error can be expressed as the difference in the distance traveled between these two paths:

$$e_i = (1 + \cos\theta)\left(Z_i^f - Z\right), \tag{3}$$

where $Z_i^f = a_i x + b_i y + c_i$ is the triangular plane equation numbered i, $Z = (x^2 + y^2)/(4F)$ is the theoretical paraboloid equation, and θ is the angle between the boresight direction and the direction from a point on the reflector to the focus. The average half-path error of the reflecting surface can then be expressed as follows:

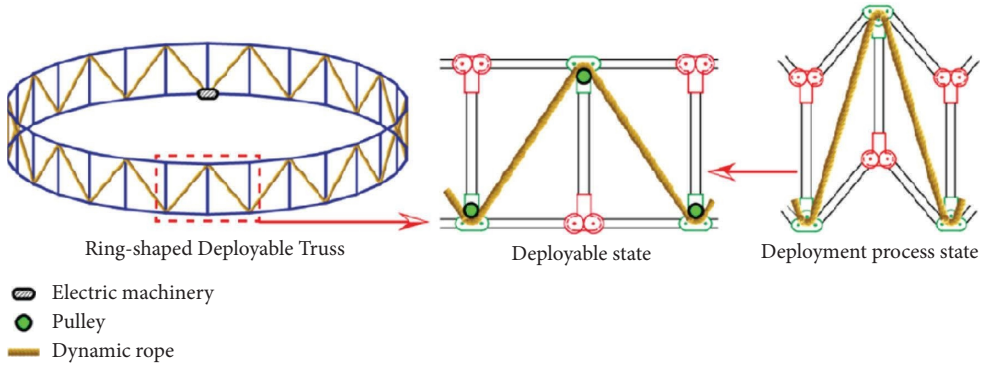

Figure 2: Deployable truss structure.

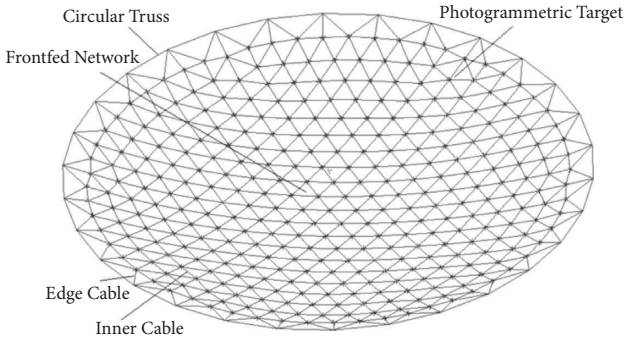

Figure 3: Measurement of the accuracy of the mesh reflector.

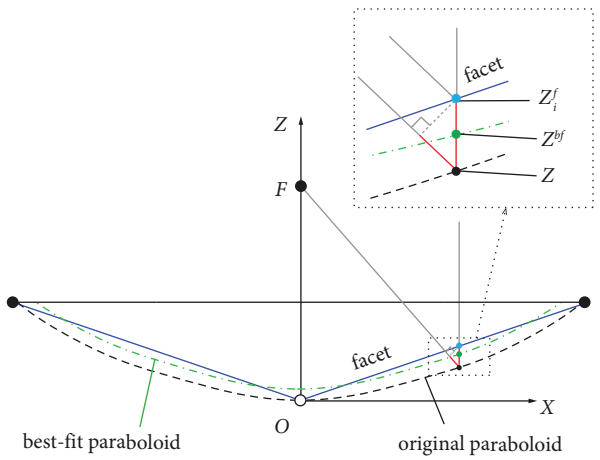

Figure 4: The error of the cable network reflector.

$$e_{\mathrm{hp}} = \sqrt{\frac{\sum_{i=1}^{N_f} \int_{A_i} (e_i/2)^2 \mathrm{d}A}{\sum_{i=1}^{N_f} \int_{A_i} \mathrm{d}A}}. \tag{4}$$

The best-fit paraboloid of the half-path error is obtained by minimizing the fitting error through shifting the original paraboloid and adjusting the focal length. This can be expressed as follows:

$$Z = \frac{\left(x^2 + y^2\right)}{\left(4F^{\mathrm{bf}}\right)} + \Delta z. \tag{5}$$

Then, the best-fit half-path error between the standard paraboloid and the network reflecting surface can be expressed as follows:

$$e_{hp}^{bf} = \sqrt{\frac{\sum_{i=1}^{N_f} \int_{A_i} \left(e_i^{bf}/2\right)^2 \mathrm{d}A}{\sum_{i=1}^{N_f} \int_{A_i} \mathrm{d}A}}, \tag{6}$$

$$e_i^{\mathrm{bf}} = \left(1 + \cos\theta^{bf}\right)\left(Z_i^f - Z^{bf}\right).$$

The parameters F^{bf} and ΔZ can be determined by solving the partial derivatives of the error function e_{hp}^{bf} with respect to F and z and setting them equal to zero to find the values of F and z that minimize the error e_{hp}^{bf}.

Due to the analysis described above, to reduce the complexity of surface adjustment, an engineering surface is proposed to approximate the manufactured surface instead of the theoretical surface. The improved error-based surface adjustment method can be optimized in the following steps:

Step 1: Using photogrammetric methods, the surfaces of the circular antenna are measured when it is placed in both forward and reverse orientations. The average of these two measurements is calculated to obtain the initial gravity-free manufacturing surface of the reflective surface $S(\Delta_1, \Delta_2, \Delta_3)$. Taking into consideration the potential errors in photogrammetric measurements, error allocation has been applied to the reflective surface. Ground-based accuracy adjustment requirements have been appropriately elevated to ensure that the antenna's reflective surface meets the on-orbit integrated accuracy requirements;

Step 2: An engineering surface S_m is proposed by optimizing F^{bf} and Δz in equation (5), which approximates $S(\Delta_1, \Delta_2, \Delta_3)$ more closely than the theoretical surface s_i;

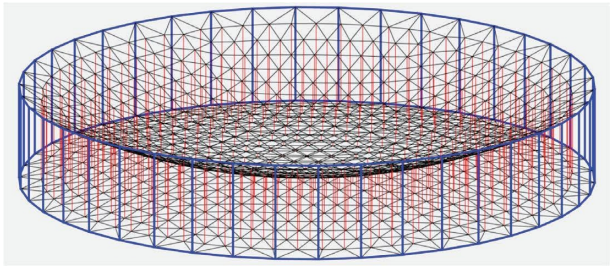

Figure 5: Model of a 20-meter loop deployable antenna reflector.

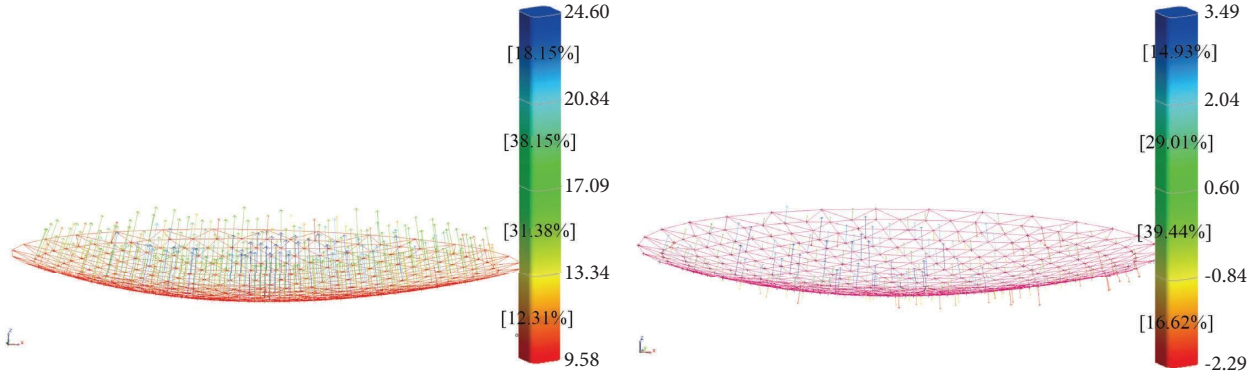

Figure 6: Surface generated by Monte Carlo method comparison between the manufactured reflector and the theoretical reflector. (a) Compare with theoretical reflector. (b) Compare with engineering reflector.

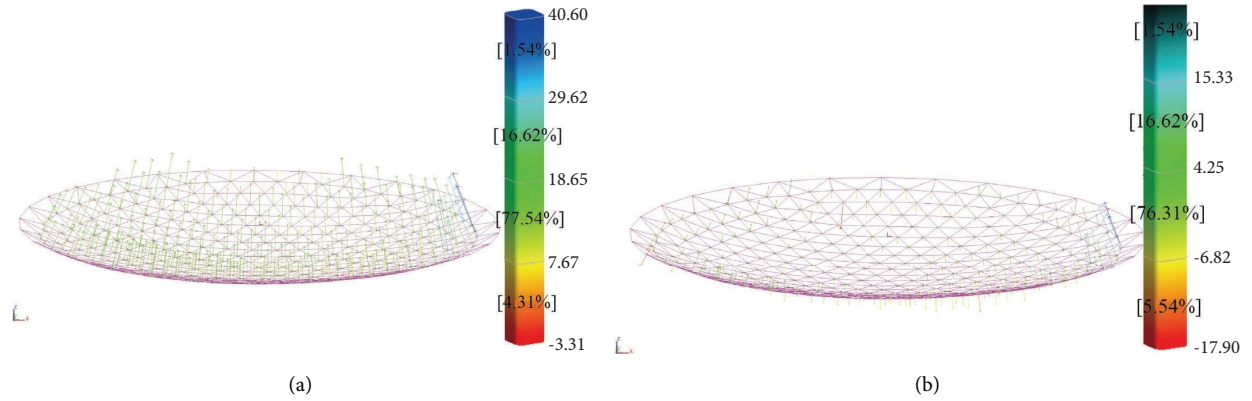

Figure 7: Photogrammetric engineering measured surface comparison of the manufacturing reflector and the engineering reflector. (a) Compare with theoretical reflector. (b) Compare with engineering reflector.

Step 3: The manufactured surface $S(\Delta_1, \Delta_2, \Delta_3)$ is adjusted to the engineering surface S_m using the improved error-based surface adjustment method.

4. Example Analysis

Taking a deployable loop antenna reflector as an example, the reflector has a circular aperture of $D = 20$ m and is composed of a ring truss with 30 units. The front and rear networks are each composed of more than a thousand ropes and connected by more than 300 tension ties. The front and rear networks are also connected to the ring truss through 90 edge cables, respectively. The entire reflector is shown in Figure 5.

Based on actual engineering experience, it is estimated that the error Δ_1 of the ring deployable truss is approximately 0.2 mm, the length error Δ_2 of the front (rear) tension cable is 0.5 mm, and the length error Δ_3 of the tension array rope is 1 mm. Using the Monte Carlo method to simulate the distribution of cable errors, the manufacturing reflector

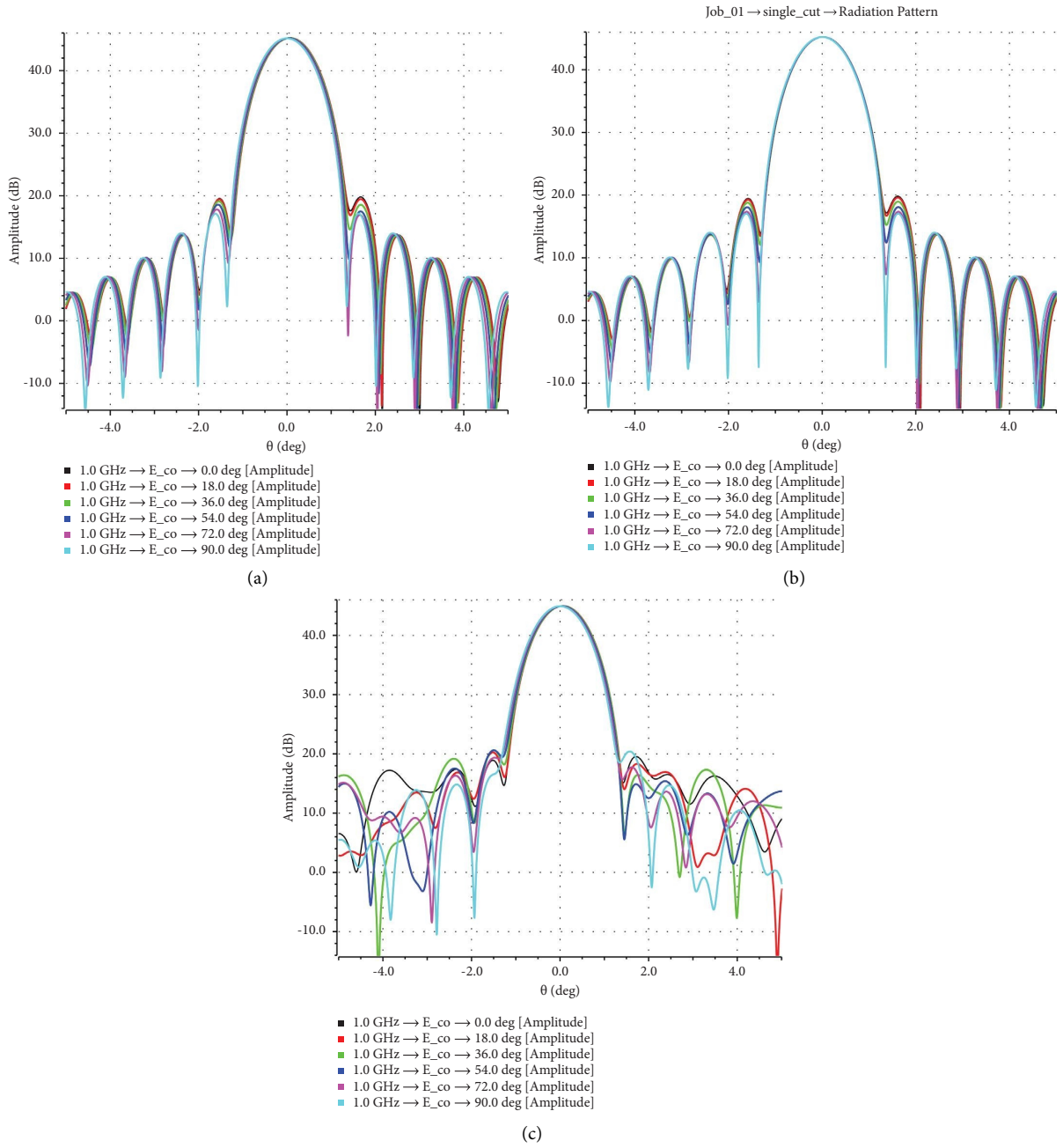

Figure 8: Electrical simulation results of focal length change and translation of the surface. (a) Engineering surface electrical simulation results (the focal length is shortened by 7.4 mm, and the z-direction translation is 18.5 mm). (b) Theoretical surface electrical simulation results. (c) Initial surface without precision adjustment electrical simulation results.

error is calculated. The resulting RMS difference between the manufactured reflector and the theoretical reflector is 17.82 mm, as illustrated in Figure 6.

According to equation (5), an engineering surface can be obtained by optimizing the focal length and translation of the theoretical paraboloid. The project surface focal length F^{bf} is 7.4 mm shorter than the theoretical focal length F, and Δz is 18.5 mm. The engineering surface approximates the manufacturing reflector much better than the theoretical surface, and the RMS error of the engineering surface and manufacturing reflector is reduced to 3.59 mm, as shown in Figure 7. Since the manufactured surface is the best-fit surface of the engineering surface, using the engineering surface as the target surface for reflector adjustment can greatly reduce the workload.

The electrical simulation results of the engineering reflector, the theoretical reflector, and the initial surface without precision adjustment using GRSAP are almost identical. As shown in Figure 8, the engineering reflector has a gain of 45.16 dB, while the theoretical reflector has a gain of 45.21 dB. The unadjusted initial network surface, as shown in Figure 7, exhibits a decrease of 44.92 dB in its electrical

simulation main lobe gain, and the side-lobe distribution is poor. Therefore, whether the adjustment target of the initial planar surface is set to the theoretical surface or the engineering surface, the difference in the adjusted electrical performance is not significant. However, the adjustment workload for the engineering surface is greatly reduced.

5. Conclusions

Due to machining and assembly errors in the manufacturing process of the large deployable antenna reflector, the final product may deviate significantly from the theoretical surface. To ensure that the manufactured reflector is close to the theoretical reflector, adjustments must be made to align the actual reflector profile with the theoretical reflector. This study proposes an optimization method that replaces the theoretical reflector with an engineering reflector. By changing the reflector adjustment target of the front tension network from the theoretical reflector to the engineering reflector, the workload of reflector adjustment can be significantly reduced, while maintaining almost unchanged electrical simulation results.

Data Availability

The data that support the findings of this study are available upon request from the corresponding author (624293993@qq.com).

Conflicts of Interest

The authors declare that they have no conflicts of interest.

Acknowledgments

Funding for this research was provided by the National Natural Science Foundation of China (grant no. 114021196). The authors would like to acknowledge their support in providing resources, equipment, and personnel necessary for conducting the experiments and data analysis presented in this paper.

References

[1] M. W. Thomson, "The AstroMesh deployable reflector," in *Proceedings of the IUTAM-IASS Symposium on Deployable Structures: Theory and Applications*, pp. 435–446, Springer, Dordrecht, Netherlands, September 2000.

[2] Y. Rahmat-Samii, A. I. Zaghloul, and A. E. Williams, "Large deployable antennas for satellite communications," in *Proceedings of the IEEE Antennas and Propagation Society International Symposium. Transmitting Waves of Progress to the Next Millennium. 2000 Digest. Held in conjunction with: USNC/URSI National Radio Science Meeting*, vol. 2, pp. 528-529, Salt Lake City, UT, USA, July 2000.

[3] A. Meguro, S. Harada, and M. Watanabe, "Key technologies for high-accuracy large mesh antenna reflectors," *Acta Astronautica*, vol. 53, no. 11, pp. 899–908, 2003.

[4] Z. Wang, T. Li, and X. Ma, "Method for generating statically determinate cable net topology configurations of deployable mesh antennas," *Journal of Structural Engineering*, vol. 141, no. 7, Article ID 04014182, 2015.

[5] Z. Zhao, Y. Peng, and J. Yang, "Deployment dynamics of mesh antennas with a modeling method of tackling the inherent multiscale problem," in *Proceedings of the 5th Joint International Conference on Multibody System Dynamics*, Lisboa, Portugal, June 2014.

[6] S. Yuan, B. Yang, and H. Fang, "The Projecting Surface Method for improvement of surface accuracy of large deployable mesh reflectors," *Acta Astronautica*, vol. 151, pp. 678–690, 2018.

[7] S. Yuan, B. Yang, and H. Fang, "Improvement of surface accuracy for large deployable mesh reflectors," in *Proceedings of the AIAA/AAS Astrodynamics Specialist Conference*, p. 5571, South Lake Tahoe, CA, USA, August 2016.

[8] M. Thomson, "Astromesh deployable reflectors for ku and ka band commercial satellites," in *Proceedings of the 20th AIAA international communication satellite systems conference and exhibit*, p. 2032, Washington, DC, USA, May 2002.

[9] M. Tabata, M. C. Natori, T. Tashima, and T. Inoue, "Adjustment procedure of a high precision deployable mesh antenna for MUSES-B spacecraft," *Journal of Intelligent Material Systems and Structures*, vol. 8, no. 9, pp. 801–809, 1997.

[10] S. Lu, X. Qi, H. Huang, Y. Hu, and B. Li, "Accuracy adjustment method of cable net surface for large Space deployable antenna," in *Proceedings of the 2018 IEEE International Conference on Information and Automation (ICIA)*, pp. 963–968, Fujian, China, August 2018.

[11] D. Jiejian, B. Duan, and F. Zheng, "The reflector shape adjusting methods for cable mesh deployable antenna," in *Proceedings of the 2006 1st International Symposium on Systems and Control in Aerospace and Astronautics*, pp. 4–1290, Harbin, China, January 2006.

[12] J. Du, Y. Zong, and H. Bao, "Shape adjustment of cable mesh antennas using sequential quadratic programming," *Aerospace Science and Technology*, vol. 30, no. 1, pp. PP26–32, 2013.